Available online at www.sciencedirect.com

ELSEVIER

Journal of Molecular Catalysis A: Chemical 246 (2006) 11–17

JOURNAL OF MOLECULAR CATALYSIS A: CHEMICAL

www.elsevier.com/locate/molcata

Highly reactive catalysts for aerobic thioether oxidation
The Fe-substituted polyoxometalate/hydrogen dinitrate system

Nelya M. Okun, James C. Tarr, Daniel A. Hilleshiem,
Lei Zhang, Kenneth I. Hardcastle, Craig L. Hill *

Department of Chemistry, Emory University, Atlanta, GA 30322-2210, USA

Received 10 August 2005; received in revised form 30 September 2005; accepted 4 October 2005

Abstract

A new type of polyoxometalate (POM), one with a hydrogen dinitrate group associated with a d-electron-substituted polyoxometalate, $Fe^{III}[H(ONO_2)_2]PW_{11}O_{39}{}^{5-}$ (**1**), has been developed that catalyzes highly effective aerobic sulfoxidation ($RR'S + 0.5\ O_2 \rightarrow RR'SO$) under ambient conditions (1 atm of air at room temperature). Comparison of the rates for aerobic sulfoxidation of the mustard simulant 2-chloroethyl ethyl sulfide (CEES) catalyzed by **1** and several other species reported to be catalysts for this class of reactions, including NO^+, NO_2, $(NH_4)_2Ce^{IV}(NO_3)_6$ and $Au^{III}Cl_2NO_3(CH_3CN)$ indicate that **1** is clearly the most effective catalyst. Conversions and selectivities for the desired sulfoxide decontamination product (CEESO in these studies) are both effectively quantitative. The low or nonexistent catalytic activity of $Fe^{II}(NO)PW_{11}O_{39}{}^{6-}$, $Fe(NO_3)_3$ and HNO_3 argues strongly that nitrosyl and nitrate derivatives of the Fe polyoxometalate and nitric acid are not species important in catalytic turnover. The techniques of single crystal X-ray diffraction, solution NMR, FTIR, TGA, DSC, cyclic voltammetry, elemental and wet chemical analyses were applied to the characterization of **1** and these are collectively consistent with the α-Keggin structure with a strongly associated hydrogen dinitrate group and a more weakly associated nitrate of crystallization.

Keywords: Selective catalytic oxidation; O_2; Polyoxometalates; Thioether; Sulfoxide; Hydrogen dinitrate; Iron

1. Introduction

The selective aerobic (O_2/air-based) oxidation of sulfides to sulfoxides is of considerable interest [1–3]. One important application is the aerobic sulfoxidation of mustard, bis(2-chloroethyl) sulfide (conventional abbreviation: "HD") (Eq. (1)). If this could be achieved under very mild conditions, it would be of major interest in protection and decontamination technologies. The sulfoxide of mustard is far less toxic than the corresponding sulfone and some mustard hydrolysis products, thus high selectivity for Eq. (1) is highly desirable. The products of:

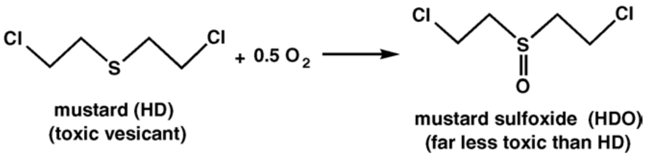

(1)

total mustard mineralization, CO_2, H_2O, HCl and inorganic sulfide or sulfur, would be quite desirable, but this complex and challenging overall transformation cannot be achieved by any system in the dark. Furthermore, even photocatalytic mineralization systems would be questionably fast enough to be effective [4]. Eq. (1) is attractive for two additional reasons: it is atom efficient and it is green (no byproducts, etc.). Recently, we and other research groups have reported several catalytic systems for aerobic sulfoxidation in the absence of light [2,5–15], but some are based solely on generation of gaseous catalysts, such as NO, which can form electron donor–acceptor complexes with sulfides or NO_2 [5,6]. Unfortunately such catalytic systems would very likely deactivate quickly under conditions and environments, where they would be needed by loss of the catalytically active gaseous specie(s). Liquids and solids are practically more attractive for stability as well as logistics reasons. However, sustained high rates of catalytic turnover for Eq. (1) under ambient conditions (1 atm of air at room temperature) with liquid or solid catalysts remains elusive.

---

* Corresponding author.

1381-1169/$ – see front matter © 2005 Elsevier B.V. All rights reserved.
doi:10.1016/j.molcata.2005.10.006

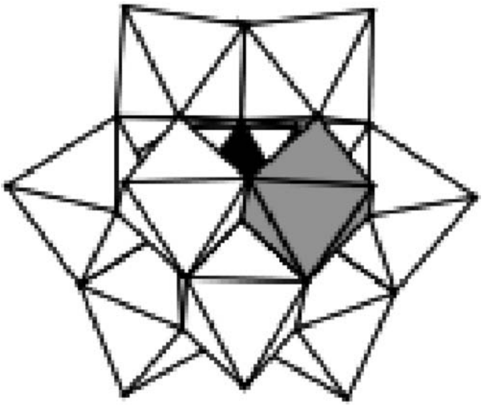

Fig. 1. Polyhedral representation of $[\alpha\text{-Fe}^{III}PW_{11}O_{39}]^{4-}$. The $PO_4{}^{3-}$ tetrahedron is shown in black; the WC_6 and FeO_6 polyhedra are shown in white and gray, respectively.

We report here the synthesis and characterization of a new iron-substituted Keggin heteropolytungstate with an associated hydrogen dinitrate group, $Fe^{III}[H(ONO_2)_2]PW_{11}O_{39}{}^{5-}$ (**1**). The TBA_3H_2 salt (TBA: tetra-*n*-butylammonium) salt of **1**, usually containing one additional nitric acid molecule of crystallization, is quite stable and when dissolved in aprotic solvents, such as acetonitrile, is the most active catalyst to date for the aerobic (air-only) sulfoxidation of 2-chloroethyl ethyl sulfide (CEES). In a thorough recent study, Khenkin and Neumann proposed the intermediacy of $N^VO_2[H_4PV_2Mo_{10}O_{40}]$ in the oxidation of alkylarenes by nitrate salts in acetic acid [16]. CEES is the best and most frequently used mustard simulant and repeated studies by our laboratory in collaboration with others have shown that CEES and mustard are oxidized at quite similar rates. In dramatic contrast to **1**, $Fe^{III}PW_{11}O_{39}{}^{n-}$ (Fig. 1) and related Fe-substituted polytungstates in the presence of only nitrate are ineffective catalysts for selective aerobic sulfoxidation. These points are investigated in conjunction with the characterization of **1**.

2. Experimental

2.1. Materials and methods

NO_2BF_4, $NOPF_6$, $(NH_4)_2Ce^{IV}(NO_3)_6$, $Fe(NO_3)_3\cdot 9H_2O$, $Ti(NO_3)_4$, the mustard simulant 2-chloroethyl ethyl sulfide and the internal standard used in quantifying product distributions by gas chromatography (1,3-dichlorobenzene) were commercial samples, $\alpha\text{-}Na_7PW_{11}O_{39}\cdot nH_2O$ [17], $Au^{III}Cl_2NO_3(CH_3CN)$ [7] and $TBA_6Fe^{II}(NO)PW_{11}O_{39}$ [18], were prepared by the literature procedures. $TBA_4Fe(H_2O)PW_{11}O_{39}\cdot nH_2O$ was prepared by cation metathesis of an aqueous solution of $Na_4Fe(H_2O)PW_{11}O_{39}\cdot nH_2O$ made by the literature method [19]. Thermogravimetric analysis (TGA) and differential scanning calorimetry (DSC) were performed on Instrument Specialists Incorporated (ISI) TGA 1000 units and DSC 550 units, respectively. Cyclic voltammograms were recorded using a glassy carbon working electrode, a Pt wire counter electrode and a $AgNO_3$ (acetonitrile)/Ag reference electrode on Princeton Applied Research potentiostat VersaStat™ II. The infrared spectra were recorded on a Nicolet™ 6700 FT-IR spectrometer from Thermo Electron. Oxidation products were identified by gas chromatography–mass spectrometry (GC–MS; Hewlett Packard 5890 series II gas chromatograph connected to a Hewlett Packard 5971 mass selective detector) and quantified by gas chromatography (GC; Hewlett Packard 5890 series gas chromatograph equipped with a flame ionization detector, 5% phenyl methyl silicone capillary column, N_2 carrier gas and a Hewlett Packard 3390A series integrator). Elemental analyses were performed by Atlantic Microlab Inc. (Atlanta, GA) for C, H, N (and O by pyrolysis) and by Desert Analytics (Tucson, Arizona) for the other elements; W was checked again by Kanti Laboratories (Mississauga, Canada).

2.2. Synthesis and characterization of $TBA_3H_2Fe^{III}[H(ONO_2)_2]PW_{11}O_{39}\cdot(HNO_3)$ (TBA_3H_2**1**)

Solid $\alpha\text{-}Na_7PW_{11}O_{39}\cdot 74H_2O$ (10 g, ca. 3.4 mmol) is dissolved in 100 mL of deionized water. To this solution, tetra-*n*-butylammonium (TBA) bromide (40 g, ca. 124 mmol) dissolved in 80 mL of deionized water is added. The mixture is stirred for 30 min at room temperature. The resulting precipitate (ca. 14.7 g) is separated by filtration, redissolved in 150 mL of acetonitrile, to which solid $Fe(NO_3)_3\cdot 9H_2O$ (1.6 g, 4.0 mmol) is added with vigorous stirring. A dark reddish-brown solution and a small amount of oily precipitate are formed. After 20 min, the solution is separated from the oily product, filtered through the fine filter paper (Fisherbrand P2) to remove the suspended precipitate, stirred for 1.5 h at ambient temperature and re-filtered through the P2 paper (it is essential to remove the oily product and any other insoluble material before crystallization). The filtrate, a clear orange solution, is left in air and light green crystals (5.8 g; 45% yield) are produced. The source of the protons in the hydrogen dinitrate and nitric acid moieties of the isolated crystalline complex is not certain but they probably derive from the hydrolysis of $Fe(NO_3)_3\cdot 9H_2O$ [20]. *Note:* these crystals crumble to a powder and the color changes from light green to yellow if they are dried in vacuo for several hours or if they are stored in air with high humidity at ambient temperature. Garbett et al. report this behavior is common for coordination compounds with nitric acid bonded to the nitrate ligand(s) [21]. IR (1% sample in KCl, 2500–500 cm^{-1}): 1620 (w), 1482 (m, sh), 1383 (s), 1151 (s), 1067 (s), 1022 (w), 965 (s), 891 (m), 815 (s), 668 (w), 591 (w) and 515 (m). *Note:* KBr is not used because there is a slow reaction between **1** and bromide ions from the KBr matrix. Anal. Calcd. For $TBA_3H_2Fe^{III}[H(ONO_2)_2]PW_{11}O_{39}\cdot(HNO_3)$ CH_3CN: C, 16.27; Fe, 1.50; H, 3.20; N, 2.60; O, 20.0; P, 0.85; W, 54.78. Found: C, 16.27; Fe, 1.51; H, 3.14; N, 2.65; O, 20.80; P, 0.84; W, 54.78. FW: 3691.5. Thermogravimetric analysis and differential scanning calorimetry curves indicate that the weakly associated HNO_3 of crystallization is lost at ca. 105 °C (2.0%; calc. 1.65%) and the hydrogen dinitrate group is lost at ca. 200 °C (TGA and DSC data are in the Supplementary Information). We sought to characterize **1** by X-ray crystallography but the mono-substituted α-Keggin complex was disordered in the solid state, as mono-substituted α-Keggin complexes invariably are and as a consequence the terminal ligation on the Fe site (12-fold disordered) could not be determined by this technique. The crystal growth and crystallography are described in Section 2.3. The $[H(ONO_2)_2]^-$ and HNO_3 moieties were both distinctly indicated by vibrational spectra and cyclic voltammetry (see Section 3.2).

2.3. X-ray diffraction studies on $TBA_3H_2Fe^{III}[H(ONO_2)_2PW_{11}O_{39}{\cdot}HNO_3$ (TBA_3H_2**1**)

A suitable crystal of **1**, prepared exactly as described above in the bulk synthesis, was coated with Paratone N oil, suspended in a small fiber loop and placed in a cooled nitrogen gas stream at 173 K on a Bruker D8 SMART APEX CCD sealed tube diffractometer with graphite monochromated Mo Kα (0.71073 Å) radiation. Data were measured using a series of combinations of phi and omega scans with 10 s frame exposures and 0.3° frame widths. Data collection, indexing and initial cell refinements were all carried out using SMART [22] software and frame integration and final cell refinements were done using SAINT [23] software. The final cell parameters were determined from least-squares refinement on 5892 reflections. The SADABS [24] program was used to carry out absorption corrections. The structure was solved using Direct methods and difference Fourier techniques (SHELXTL, V5.10). Only the P and W atoms were refined anisotropically; hydrogen atoms were positioned by using the HFIX command in SHELXTL and incorporated as riding atoms in the final cycles of least-squares refinement. Scattering factors and anomalous dispersion corrections are taken from the *International Tables for X-ray Crystallography* [25]. Structure solution, refinement, graphics and generation of publication materials were performed by using SHELXTL, V5.10 software. The crystal structure consists of one Keggin POM and three tetra-*n*-butyl ammonium ions per asymmetric unit. One iron atom shares the 12 metal atom sites with 11 tungsten atoms and is completely disordered within the Keggin unit. Additional details of data collection and structure-refinement are summarized in Table 1 and a thermal ellipsoid plot is given in the Supplementary Information. Unfortunately two additional X-ray structure determinations of **1** provided the same data (were identically disordered).

2.4. Procedure for catalytic reactions

2-Chloroethyl ethyl sulfide (0.875 mmol), catalyst (quantity given in column 2 in Table 2), 1 atm of air, 0.876 mmol of 1,3-dichlorobenzene (internal standard) were stirred in 2.3 mL of acetonitrile at 25 °C for the times in Table 2 in a 20 mL vial with a headspace of 21.5 mL. The products were then analyzed by gas chromatography as described above (Section 2.1).

2.5. Establishment of stoichiometry of the overall catalyzed reactions

The stoichiometry of the overall catalyzed reaction was confirmed to be the desired (atom efficient) "dioxygenase" one analogous to Eq. (1), namely CEES + $\frac{1}{2}O_2 \rightarrow$ CEESO. This was established by simultaneously quantifying both O_2 by digital manometry and CEES and CEESO by gas chromatography using internal standard methods. In addition, the full time dependence of this stoichiometry to high conversions has been determined and the data are plotted in S8 in the Supplementary Information. This 2:1 dioxygenase stoichiometry is operable at both low and high conversions.

Table 1
Crystallographic data and structure-refinement parameters for $TBA_3H_2Fe^{III}[H(ONO_2)_2]PW_{11}O_{39}^{5-}$ (**1**)

Formula	$TBA_3HFe^{III}(OH_2)PW_{11}O_{39}$
M_r [g mol^{-1}]	3476.54
Crystal system	Triclinic space group *Plbar*
a [Å]	13.7390(10)
b [Å]	15.4413(11)
c [Å]	19.3947(14)
α [°]	95.351(2)
β [°]	93.030(2)
γ [°]	90.864(2)
V [Å^3]	4090.1(5)
[K]	173(2)
Z	2
$d_{\mathrm{calcd.}}$ [mg m^{-3}]	2.823
Crystal size [mm]	0.34 × 0.15 × 0.15
Absorption coefficient [mm^{-1}]	15.671
$2\theta_{\mathrm{limits}}$ (°)	1.48–28.39
Data/restraints/parameter	20394/0/518
Absorption correction	SADABS
R_1/wR_2	0.0892/0.2288
Goodness of fit	1.032
Largest residuals [eÅ^3]	+9.230/−5.707

Full positional disorder precluded location/identification of the $[H(ONO_2)_2]^{1-}$ unit.

3. Results and discussion

3.1. Evaluation of catalysts for aerobic sulfoxidation

Table 2 compares the reactivities of a new ferric heteropolytungstate, $TBA_3H_2Fe^{III}[H(ONO_2)_2]PW_{11}O_{39}$, as a nitric acid solvate, TBA_3H_2**1** and the many other previously reported catalysts for aerobic sulfoxidation under ambient conditions (1 atm of air at room temperature in acetonitrile solution) using the fairly unreactive mustard simulant, 2-chloroethyl ethyl sulfide, CEES, as the substrate [26]. TBA_3H_2**1** is an unusually challenging complex to rigorously characterize structurally and a discussion of this effort in Section 3.2 follows from the discussion of reactivity in this section. The conversion in most reactions was kept relatively low so rates of the different systems could be more meaningfully compared. *Importantly, the selectivity in most of the systems, including the best system, **1**, is effectively quantitative for sulfoxide throughout the reaction and conversions in most of these catalytic reactions, including those with **1**, also approach 100*%. The control with only CEES present (no catalyst of any kind) produced no sulfoxide (CEESO) or other organic product. The following species reported to be catalysts for (or closely related to catalytically competent species) for aerobic sulfoxidation, each evaluated separately and in duplicate under identical turnover reaction conditions, proved to far less active than **1**: NO^+, NO_2^+, NO_3^- in three different complexes,

Table 2

Aerobic oxidation of 2-chloroethyl ethyl sulfide (CEES) in acetonitrile by a range of homogeneous catalysts under ambient conditions[a]

	Catalyst	[Catalyst] (mmol)[b]	Storage time (days)[c]	Conversion[d] (%)	TOF[e]
1	$NOPF_6$	0.005	–	2.8	0.1
2	NO_2BF_4	0.005	–	2.5	0.1
3	$(NH_4)_2Ce^{IV}(NO_3)_6$	0.006	–	28.0	1.2
4	$Au^{III}Cl_2NO_3(CH_3CN)$	0.005	–	∼0	∼0
5	$Ti(NO_3)_4$	0.008	–	29.5	0.8
6	$TBA_6Fe^{II}(NO)PW_{11}O_{39}$	0.005	–	0	0
7	$Fe(NO_3)_3{\cdot}9H_2O$	0.005	–	0	0
8	$TBA_4Fe(H_2O)PW_{11}O_{39}{\cdot}nH_2O$	0.005	–	0	0
9	HNO_3	0.005 [f]	–	4.0	0.2
10	$TBA_4Fe(H_2O)PW_{11}O_{39} + TBANO_3$ [g]	0.005	–	0	0
11	$TBA_4Fe(H_2O)PW_{11}O_{39} + TBANO_2$ [h]	0.005	–	0	0
12	$TBA_4Fe(H_2O)PW_{11}O_{39} + HNO_3$[i]	0.005	–	3.5	0.2
13	$TBA_4Fe(H_2O)PW_{11}O_{39} + TBANO_3 + H^+$[j]	0.0045	–	70	40
14	$TBA_3H_2\mathbf{1}$[k]	0.005	–	92.8	4.1
15	$TBA_3H_2\mathbf{1}$[k]	0.005	30	56.5	2.5
16	$TBA_3H_2\mathbf{1}$[k]	0.005	54	44.0	1.9
17	$TBA_3H_2\mathbf{1}$[k]	0.005	215	19.0	0.8
18	$TBA_3H_2\mathbf{1}$,[k] small headspace [l]	0.005	54	22.0	1.0
19	$TBA_3H_2\mathbf{1}$,[k] large headspace [m]	0.005	54	9.5	0.4
20	$TBA_3H_2\mathbf{1}$[k] + 2,6-di-*t*-butylpyridine[n]	0.012	0	0	0
21	$TBA_{12\text{-}x}K_x\{[Fe^{III}(OH_2)(HNO_3)]_3\text{-}(A\text{-}\alpha\text{-}PW_9O_{34})_2\}^{12-}$ [o]	0.005	0	0	0

[a] *General conditions:* 0.875 mmol of CEES, catalyst (quantity given in column 2), 1 atm of air, 0.876 mmol of 1,3-dichlorobenzene (internal standard) were stirred in 2.3 mL of acetonitrile at 25 °C for 40 h in the 20 mL vial with headspace of 21.5 mL.

[b] mmol of total catalyst present during turnover.

[c] Days POM stored while being exposed to daylight.

[d] Conversion (%) = (mol of CEES consumed/mol of initial CEES) × 100.

[e] Turnover frequency = (moles of CEESO/moles of POM) × (reaction time (20 h))$^{-1}$.

[f] $[HNO_3]$ (mmol).

[g] $TBA_4Fe(H_2O)PW_{11}O_{39}$ (0.005 mmol) + $TBANO_3$ (0.005 mmol).

[h] $TBA_4Fe(H_2O)PW_{11}O_{39}$ (0.005 mmol) + $TBANO_2$ (0.005 mmol).

[i] $TBA_4Fe(H_2O)PW_{11}O_{39}$ (0.005 mmol) + HNO_3 (0.005 mmol).

[j] $TBA_4Fe(H_2O)PW_{11}O_{39}$ (0.005 mmol) + $TBANO_3$ (0.0105 mmol) + *p*-toluenesulfonic acid (0.0108 mmol).

[k] $\mathbf{1} = [Fe^{III}[H(ONO_2)_2]PW_{11}O_{39}]^{5-}$.

[l] Oxidation conducted with headspace of 0.8 mL.

[m] Oxidation conducted with headspace of 59.5 mL.

[n] $TBA_3H_2\mathbf{1}$ (0.012 mmol) + 2,6-di-*t*-butylpyridine (0.10 mmol).

[o] Complex was prepared by adding $TBANO_3$ to a sample of $K_9[Fe^{III}(OH_2)]_3(A\text{-}\alpha\text{-}PW_9O_{34})_2$ (prepared according to Ref. [10]). Anal. Calcd.: C, 22.07; Fe, 2.41; H, 4.23; N, 2.21; O, 18.37; P, 0.89; W, 47.51. Found: C, 22.17; Fe, 2.45; H, 4.30; N, 2.25; O, 18.80; P, 0.84; W, 47.78. FW: 6965.8. See Fig. S4 in the Supplementary Information for infrared data.

HNO_3 (Table 2, entries 1, 2, 3–5 and 9, respectively) and NO_2^- (see Table 2, entry 11) [5,27]. Ceric ammonium sulfate, the most effective catalyst for the aerobic oxidation of sulfides to sulfoxides prior to 1995 [28] is active under the conditions in Table 2 but significantly less so than several catalysts developed more recently (entry 3). The thoroughly investigated d^8 Au(III) nitrate complexes are active, but again, less so than more recently developed catalysts (entry 4) [2,7,8]. $Ti(NO_3)_4$, perhaps the best studied catalytically active covalent nitrate complex [29] was also evaluated. It clearly catalyzes aerobic sulfoxidation, but again, it is not the most active catalyst in this study (Table 2, entry 5).

Iron(II)–nitrosyl heteropolytungstates have been prepared and demonstrated to be catalysts for the electroreduction of NO_2^- and NO to NH_3 [18]. Further, both Fe(II) heteropolytungstates and NO could be intermediates under the experimental conditions used in this study (Table 2). As a consequence, we prepared $Fe^{II}(NO)PW_{11}O_{39}{}^{6-}$ and evaluated it for aerobic sulfoxidation activity under the same conditions as for the other compounds (Table 2, entry 6). It proved to be catalytically inactive ruling out Fe–NO species as viable intermediates during catalytic sulfoxidation by the best catalyst, **1**.

Bosch and Kochi established that NO_2, which is in equilibrium with N_2O_4 (bp 21 °C at 1 atm) [30], catalyzes aerobic sulfoxidation under mild conditions. NO also readily forms NO_2 under the reaction conditions (Table 2) via $NO + \frac{1}{2}O_2 \rightarrow 2\,NO_2$. While control reactions with various authentic NO_x species were evaluated (see above), an additional experiment addressing the possible catalytic role of any gaseous specie, most obviously NO_2, in the reactions catalyzed by **1** in Table 2 was conducted. Specifically, the reaction catalyzed by **1** was run under two distinct conditions, one using almost no gaseous headspace over the catalytic solution in the reaction vessel (Table 2, entry 17) and one using a very large headspace (Table 2, entry 18). These reactions did not give dramatically different results (the small headspace reaction is two to three times faster and has comparably larger conversions). However, this difference is sufficiently great to argue that some volatile NO_x intermediate may be catalytically competent; this species would be present in substantially lower concentration in the solution for the high headspace reaction. It is likely the ratio of rates (small versus large headspace) would be far larger if only some NO_x specie was the catalyst.

Catalytic aerobic sulfoxidation by **1** is co-catalyzed by acid. While **1** itself is only modestly acidic, if it is titrated by an excess of the proton-specific base, 2,6-di-*t*-butylpyridine, the catalytic aerobic sulfoxidation reactivity is lost (Table 2, entry 20). This most likely reflects and thus constitutes some evidence for the intermediacy of peroxy species [31,32]. However, it should be noted that oxidation of organic sulfides by anhydrous H_2O_2 using percarbonate in glacial acetic acid is independent of the acidity of the medium [33].

To confirm that sulfides other than CEES are rapidly, selectively and quantitatively converted to their corresponding sulfoxides by **1**, several reactions using tetrahydrothiophene (THT) as the sulfide reactant in place of CEES were also evaluated. As expected, given the far higher reactivity of THT toward electrophilic oxygenation agents [26,32,34], rapid selective conversion of THT to the sulfoxide THTO was demonstrated (see Table S6 in the Supplementary Information).

Significantly, if water is used as the solvent in the preparation of **1** instead of acetonitrile, a catalytically inactive complex results. Water likely disrupts the NO_x ligands on the POM Fe center or otherwise prevents formation of the associated NO_x moieties essential for the reactivity in **1** (see Section 3.2). The structure of the Fe POM is also an important factor in reactivity; the acetonitrile-soluble $TBA_{12-x}K_x$ salt of $\{[Fe^{III}(OH_2)(HNO_3)]_3(A\text{-}\alpha\text{-}PW_9O_{34})_2\}^{12-}$, was prepared by simple metathesis from the well-characterized complex $[(Fe^{III}(OH_2)_2)_3(A\text{-}\alpha\text{-}PW_9O_{34})_2]^{9-}$ [10,15], following the same protocol used to prepare **1**. It proved to be completely inactive under the conditions in (Table 2, final entry).

3.2. *Synthesis and characterization of the optimally active aerobic sulfoxidation catalyst, 1*

The extremely active aerobic sulfide oxidation catalyst, TBA_3H_2**1**, is reproducibly formed only when the TBA salt of the defect (lacunary) polytungstate, $\alpha\text{-}PW_{11}O_{39}{}^{7-}$ is treated with $Fe(NO_3)_3$ in nonaqueous media and specifically in acetonitrile. Given the unusual activity of **1**, considerable effort was made to characterize this complex in its isolable but active form along with several closely related complexes and synthetic precursors. The techniques of single crystal X-ray diffraction, solution NMR, FTIR, TGA, DSC, cyclic voltammetry, elemental analysis and three wet chemical analyses were used. Most of the data are presented in the Supplementary Information. Unfortunately, the paramagnetism of **1** precluded acquisition of informative NMR spectra. In addition, three different single crystal X-ray structure determinations of **1** all produced the expected positionally disordered crystals (each metal center is 1/12 Fe and 11/12 W). This is not surprising given that all mono-substituted α-Keggin complexes to date have been so disordered in the solid state. On the positive side, the X-ray crystallography established that the reactive solid was, in fact, an α-Keggin complex (see S7 in the Supplementary Information). On the negative side, the disorder precluded unequivocal structural identification of the NO_x species associated with the $\alpha\text{-}Fe^{III}PW_{11}O_{39}{}^{4-}$ unit.

Despite this problem, however, the presence and nature of the NO_x groups in TBA_3H_2**1** was confirmed and addressed by the several lines of direct and indirect evidence. First, both the Brown Ring test (S1.1 in the Supplementary Information) and the Brucine test (S1.2 in the Supplementary Information) indicated the presence of nitrate in catalytically active **1**. Second, a titration and gravimetric analysis using nitron (4,5-dihydro-l,4-diphenyl-3,5-phenylimino-l,l,4-triazole) (S1.3 in the Supplementary Information) indicated that each molecule of **1** contains 5.04% nitrate (of 0.105 g of TBA_3H_2**1**) or about 3 nitrate equivalents per molecule of **1**. This is consistent with one hydrogen dinitrate and one weakly associated third equivalent of nitric acid per polytungstate unit from the elemental analyses. Third, the thermal data (TGA and in particular, the DSC data; Fig. S2a and b in the Supplementary Information) also indicate the loss of one equivalent of weakly associated nitrate at 105 °C (2.0%; calculated 1.65%) and the two equivalents in the hydrogen dinitrate group at ca. 200 °C. Thus three independent experimental efforts all implicate the presence of one hydrogen dinitrate unit and one weakly associated nitric acid per α-Fe $PW_{11}O_{39}{}^{4-}$ unit: the elemental analysis, the nitron titration and gravimetric analysis and the DSC/TGA data.

The fourth type of experimental data bearing on the NO_x ligands in **1** derives from cyclic voltammetry (CV). Three POM derivatives, $TBA_4H_3PW_{11}O_{39}$, $TBA_4Fe(H_2O)PW_{11}O_{39}$ and TBA_3H_2**1** were examined by CV in the same solvent used in catalysis—acetonitrile (Fig. S3 in the Supplementary Information). The peaks for the Fe(III/II) couple and the more negative W(VI/V) peaks from reduction of the polytungstate framework are clear and shift when nitrate is present (i.e. in TBA_3H_2**1** relative to $TBA_4Fe(H_2O)PW_{11}O_{39}$). It is apparent that the Fe(III/II) couple is the one most impacted by the presence of NO_x, consistent with coordination of some NO_x moiety to the Fe center. However, it is also likely that NO_x ligands are in dynamic exchange in acetonitrile and a kinetically viable population of NO_x could well be dissociated from Fe (freely diffusing in solution) under catalytic turnover conditions.

The fifth and most structurally informative line of experimental evidence addressing the nature of NO_x in the active catalyst, **1**, is vibrational spectroscopy. The key data are presented in Fig. 2 [35–44]. A careful comparison of the FTIR spectra of key POM species (TBA_3H_2**1** under varying conditions and $TBA_4Fe(H_2O)PW_{11}O_{39}$) with catalytic aerobic sulfoxidation activity (conditions in Table 2) lead to several conclusions. Clearly, several NO_x species can be ruled out because their vibrational signatures (as well as their assessed activities in Table 2 above) preclude their presence. These include nitrite ($NO_2{}^-$), either free or in any association mode, NO_2 (g), metal–nitro (M–NO_2) species, either terminal or bridging, monodentate nitrate (M–O–NO_2) and bidentate nitrate (M–O_2NO). TBA_3H_2**1** has peaks at -1383, 1481 and 1665 cm^{-1}. Again, these are most consistent with the presence of the hydrogen dinitrate moiety $[H(ONO_2)_2]^-$ [45–47]. The behavior of hydrogen dinitrate [47]

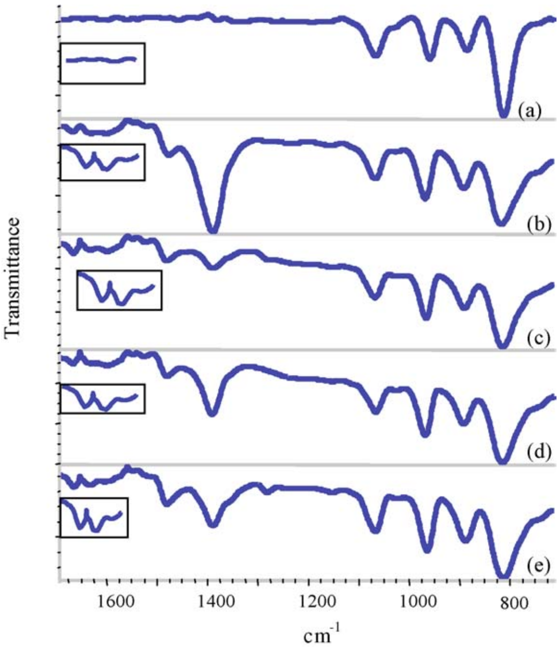

Fig. 2. Infrared spectra of $TBA_4Fe(H_2O)PW_{11}O_{39}\cdot 2H_2O$ (a); TBA_3H_2**1** (b); TBA_3H_2**1**, dried in vacuum or after 215 days of storage (c); TBA_3H_2**1**, dried in vacuum and then treated with dry HNO_3 (d); TBA_3H_2**1** dried in vacuum and then recrystallized from HNO_3 solution in acetonitrile (e).

as well as its structure in solution and in the solid state from X-ray diffraction [37,48,49], inelastic neutron scattering [50] and vibrational (both IR and Raman) spectroscopy [35–37] are documented. When nitric acid bonds to nitrate ion forming the hydrogen dinitrate ion, the generic μ_3 band of the nitrate moiety (typically $-1383\,\mathrm{cm}^{-1}$) usually vanishes [46]. When **1** is dried in vacuum at RT for at least 48 h, the μ_3 and $1633\,\mathrm{cm}^{-1}$ bands diminish, whereas the μ_4 absorption bands at 1481 and $1665\,\mathrm{cm}^{-1}$ are minimally affected (Fig. 2c). The μ_3 band is restored after treating the dried sample of **1** with dry HNO_3 or recrystallizing it from nitric acid solution in acetonitrile [51] and again, the μ_4 bands at 1481 and $1665\,\mathrm{cm}^{-1}$ are not effected (Fig. 2d and e). The analytical and DSC/TGA data elaborated in Section 3.1, the control reactivities studies (Table 2) and the vibrational analysis here are all mutually confirmatory and consistent with the presence of hydrogen dinitrate in TBA_3H_2**1**.

Significantly, catalytic activity correlates closely with the presence of the full set of bands associated with hydrogen dinitrate. It does not correlate with bands of any monomeric nitrate alone. In addition, the presence of the Fe-containing POM is essential (again, there is little catalytic activity if only NO_x species are present).

From the reactivities in Table 2, the gas headspace experiment and other data, it is apparent that catalysis by this highly effective system, **1**, is quite complex and would necessarily demand a considerable number of experiments to definitely elucidate the mechanism. Having made this point evident, we determined that the rates for sulfoxidation under the conditions in Table 2 are first-order in **1** over a considerable concentration range and 9 data points (see Fig. S5B) but interpretation of this should be conducted with caution. More easily interpreted is the fact that the reaction rate is zero order in O_2, at least under the conditions in this study, indicating that steps other than reoxidation are rate limiting.

4. Conclusions

The most reactive catalyst yet for selective aerobic sulfoxidation, $Fe^{III}[H(ONO_2)_2]PW_{11}O_{39}{}^{5-}$ (**1**), has been identified and investigated. Although NMR and X-ray crystallography, the two most definitive structural methods, can not be used to characterize **1** because of paramagnetism and positional disorder in the solid state, respectively, vibrational spectroscopy in conjunction with several wet chemical analyses, thermal studies, elemental analyses and the correlation of this data with catalytic activity for air-oxidation of 2-chloroethyl ethyl sulfide and tetrahydrothiophene implicate the presence of the hydrogen dinitrate groups in the optimally active and investigated form of the catalyst, TBA_3H_2**1**. Other approaches to further elucidate the precise structures of the NO_x groups in **1** are being pursued including the use of β-$Fe(H_2O)PW_{11}O_{39}{}^{4-}$ in place of the a isomer present in **1**. The β isomers are far less prone than the α isomers to positionally disordered crystals in the solid state.

Acknowledgments

We wish to thank the Army Research Office (Grant numbers DAAD 19-01-1-0593 and currently W911NF-05-1-0200) and the Natick Soldier Center/Battelle for funding and Travis M. Anderson for help with manuscript preparation.

Appendix A. Supplementary data

Supplementary data associated with this article can be found, in the online version, at doi:10.1016/j.molcata.2005.10.006.

References

[1] S.-I. Ozaki, P.R. Ortiz de Montellano, J. Am. Chem. Soc. 117 (1995) 7056–7064.
[2] E. Boring, Y. Geletii, C.L. Hill, in: L.I. Simandi (Ed.), Catalytic Activation of Dioxygen: Catalysts for Selective Aerobic Oxidation under Ambient Conditions. Thioether Sulfoxidation Catalyzed by Gold Complexes, Kluwer, Dordrecht, 2001.
[3] M.S. Sigman, D.R. Jensen, S. Rajaram, Curr. Opin. Drug Discov. Dev. 5 (6) (2002) 860–869.
[4] N. Somasundaram, C. Srinivasan, J. Photochem. Photobiol. A Chem. 115 (2) (1998) 169–173.
[5] E. Bosch, J.K. Kochi, J. Org. Chem. 60 (1995) 3172–3183.
[6] E. Bosch, J.K. Kochi, J. Am. Chem. Soc. 118 (1996) 1319–1329.
[7] E. Boring, Y.V. Geletii, C.L. Hill, J. Am. Chem. Soc. 123 (2001) 1625–1635.
[8] E. Boring, Y. Geletii, C.L. Hill, J. Mol. Catal. A Chem. 176 (2001) 49–63.
[9] S.E. Martin, L.I. Rossi, Tetrahedron Lett. 42 (2001) 7147–7151.
[10] N.M. Okun, T.M. Anderson, C.L. Hill, J. Am. Chem. Soc. 125 (2003) 3194–3195.
[11] N.M. Okun, T.M. Anderson, C.L. Hill, J. Mol. Catal. A Chem. 197 (2003) 283–290.
[12] N.M. Okun, T.M. Anderson, K.I. Hardcastle, C.L. Hill, Inorg. Chem. 42 (2003) 6610–6612.
[13] L.I. Rossi, S.E. Martin, Appl. Catal. A 250 (2003) 271–278.

[14] R. Xu, H.C. Zeng, Chem. Mater. 15 (2003) 2040–2048.

[15] N.M. Okun, M.D. Ritorto, T.M. Anderson, R.P. Apkarian, C.L. Hill, Chem. Mater. 16 (2004) 2551–2558.

[16] A.M. Khenkin, R. Neumann, J. Am. Chem. Soc. 126 (2004) 6356–6362.

[17] R. Contant, Can. J. Chem. 65 (1987) 568–573.

[18] J.E. Toth, F.C. Anson, J. Am. Chem. Soc. 111 (1989) 2444–2451.

[19] F. Zonnevijlle, C.M. Tourne, G.F. Tourne, Inorg. Chem. 21 (1982) 2751–2757.

[20] A.V. Gorelova, L.M. Sukova, T.I. Romantseva, M.A. Kolenkova, O.P. Chernova, Zh. Neorg. Khim. 31 (1986) 2065–2068.

[21] K. Garbett, R.D. Gillard, R. Ugo, J. Chem. Soc. A (1966) 1137–1139.

[22] SMART Version 5.628, Analytical X-Ray Systems, Bruker AXS Inc., 5465 East Cheryl Parkway, Madison, WI 53711-5373, 2003.

[23] SAINT Version 6.36A, Analytical X-Ray Systems, Bruker AXS Inc., 5465 East Cheryl Parkway, Madison, WI 53711-5373, 2002.

[24] SADABS Version 2.10, G. Sheldrick, University of Gottingen, 2003.

[25] A.J.C. Wilson (Ed.), International Tables for X-ray Crystallography, vol. C, Academic Publishers, Kynoch, Dordrecht, 1992.

[26] R.D. Gall, M. Faraj, C.L. Hill, Inorg. Chem. 33 (1994) 5015–5021.

[27] E. Bosch, J.K. Kochi, in: Z.B. Alfassi (Ed.), Nitrogen Dioxide Reactivity Toward Organic Donors in the Liquid Phase: N-Centered Radicals, John Wiley & Sons, Chichester, 1998, pp. 68–128.

[28] D.P. Riley, M.R. Smith, P.E. Correa, J. Am. Chem. Soc. 110 (1988) 177–180.

[29] C.D. Garner, S.C. Wallwork, J. Chem. Soc. A (1966) 1496–1500.

[30] D.R. Lide, CRC Handbook of Chemistry and Physics, 81st ed., CRC Press, Boca Raton, FL, 2000.

[31] R.A. Sheldon, J.K. Kochi, Metal-Catalyzed Oxidations of Organic Compounds, Academic Press, New York, 1981.

[32] R.D. Gall, C.L. Hill, J.E. Walker, J. Catal. 159 (1996) 473–478.

[33] C. Karunakaran, R. Kamalam, React. Kinet. Catal. Lett. 76 (2002) 37–42.

[34] R.D. Gall, C.L. Hill, J.E. Walker, Chem. Mater. 8 (1996) 2523–2527.

[35] S. Detoni, L. Diop, R. Gunde, D. Hadz, B. Orel, A. Potier, J. Potier, Spectrochim. Acta 35A (1979) 443–454.

[36] B. Barlic, D. Hadzi, B. Orel, Spectrochim. Acta 37A (1981) 1047–1048.

[37] D.V. Pozdnyakov, V.N. Filimonov, Kinet. Katal. 14 (1973) 760–766.

[38] D. Hadzi, J. Chem. Soc. A (1962) 5128–5138.

[39] C. Addison, C.D.W. Amos, D. Sutton, J. Chem. Soc. A (1967) 808–812.

[40] C.C. Addison, N. Logan, S.C. Wallwork, C.D. Gamer, Q. Rev. 25 (1971) 289–322.

[41] C.D. Garner, I.H. Hillier, M. Guest, J. Chem. Soc. Dalton Trans. 19 (1975) 1934–1938.

[42] C.C. Addison, Chem. Rev. 80 (1980) 21–39.

[43] J.C. Fanning, J.L. Resce, G.C. Lickfield, N.E. Kotun, Inorg. Chem. 24 (1985) 2884–2889.

[44] W.H. Knoth, P.J. Domaille, R.L. Harlow, Inorg. Chem. 25 (1986) 1577–1584.

[45] B.O. Field, C.J. Hardy, Q. Rev. 18 (1964) 361–388.

[46] R.D. Gillard, R. Ugo, J. Chem. Soc. A (1966) 549–552.

[47] B.D. Faithful, R.D. Gillard, D.G. Tuck, R. Ugo, J. Chem. Soc. A (1966) 1185–1188.

[48] J.M. Williams, N. Dowling, R. Gunde, D. Hadii, B. Orel, J. Am. Chem. Soc. 98 (1976) 1581–1582.

[49] N.S. Al-Zamil, E.H.M. Evans, R.D. Gillard, D.W. James, T.E. Jankins, R.J. Lancashire, P.A. Williams, Polyhedron 1 (1982) 525–534.

[50] K.P. Brierley, J. Howard, C.J. Ludman, K. Robson, T.C. Waddington, J. Tomkinson, Chem. Phys. Lett. 59 (1978) 467–471.

[51] The vapor above HNO_3/H_2SO_4, 50:50 (v/v) solution was used as a source of dry HNO_3.